Electronic Supporting Information (ESI)

Heterometal functionalization yields improved energy density for charge carriers in nonaqueous redox flow batteries

Lauren E. VanGelder and Ellen M. Matson*

Department of Chemistry, University of Rochester, Rochester, New York 14627
Corresponding author email: matson@chem.rochester.edu

Supporting Information Table of Contents

Experimental Methods:

General Considerations. All manipulations were carried out in the absence of water and oxygen in a UniLab MBraun inert atmosphere glovebox under a dinitrogen atmosphere. Glassware was oven dried for a minimum of 4 hours and cooled in an evacuated antechamber prior to use in the drybox. Anhydrous methanol was purchased from Sigma-Aldrich and stored over activated 4 Å molecular sieves purchased from Fisher Scientific. All other solvents were dried and deoxygenated on a Glass Contour System (Pure Process Technology, LLC) and stored over activated 3 Å molecular sieves purchased from Fisher Scientific. $[NBu_4][BH_4]$ and $Ti(OCH_3)_4$ were purchased from Sigma-Aldrich and used as received. $[NBu_4][PF_6]$ was purchased from Sigma-Aldrich, recrystallized thrice using hot methanol, and stored under dynamic vacuum for a minimum of two days prior to use. $[NBu_4][TiV_5O_6(OCH_3)_{13}]$ (**1-TiV$_5$**), and $[Ti_2V_4O_5(OCH_3)_{14}]$ (**2-Ti$_2$V$_4$**) were synthesized according to previous literature.[1] Electronic absorption measurements were recorded at room temperature in anhydrous acetonitrile in a sealed 1 cm quartz cuvette with an Agilent Cary 60 UV-Vis spectrophotometer. All electrochemical experiments were conducted in the glove box using a Bio-Logic SP 150 potentiostat/galvanostat and the EC-Lab software suite.

Determining D_0 and k_0. Concentrations of **1-TiV$_5$** and **2-Ti$_2$V$_4$** used were 5 mM with 0.1 M $[NBu_4][PF_6]$ supporting electrolyte. CV measurements were carried out inside a nitrogen filled glove box (MBraun, USA) using a Bio-Logic SP 150 potentiostat/galvanostat and the EC-Lab software suite. Cyclic voltammograms were recorded using a 3 mm diameter glassy carbon working electrode (CH Instruments, USA), a Pt wire auxiliary electrode (CH Instruments, USA), and a Ag/Ag^+ non-aqueous reference electrode with 0.01 M $AgNO_3$ in 0.05 M $[NBu_4][PF_6]$ in CH_3CN (Bio-Logic). Cyclic voltammograms were *iR* compensated at 85% with impedance taken at 100 kHz using the ZIR tool included within the EC-Lab software.

The diffusion coefficient associated with each redox couple was determined by using the slope of the peak current (i_P) versus the square root of scan rate $\nu^{1/2}$. The Randles-Sevcik equation was used to estimate the diffusion coefficients from CV data. For a reversible redox couple, the peak current is given by the eq. S1;

$$i_p = 2.69 \times 10^5\, n^{3/2}\, A\, c\, D_0^{1/2}\, \nu^{1/2} \quad \text{Eq. S1}$$

In eq. S1, *n* is the number of electrons transferred; *A* is the electrode area (0.0707 cm^2 for the glassy carbon working electrode); *c* is the bulk concentration of the active species; D_0 is the diffusion coefficient of the active species; ν is the scan rate. For an irreversible redox couple, the peak current, is given by the eq. S2:

$$i_p = 2.99 \times 10^5\, n^{3/2}\, \alpha^{1/2}\, A\, c\, D_0^{1/2}\, \nu^{1/2} \quad \text{Eq. S2}$$

where α is the charge transfer coefficient (α ~ 0.5).

For the redox couples that show quasi-reversible kinetics, relationships for both reversible and irreversible redox reaction are usually employed to determine the diffusion coefficients of such redox processes. Therefore, an average value of diffusion coefficient was approximated for a quasi-reversible redox couple using both equations S1 and S2.[2-4]

The Heterogeneous Electron-Transfer Rate Constants were calculated using the Nicholson method.[5] The potential difference (ΔEp) of oxidation and reduction peaks were obtained at different scan rates. The transfer parameter, ψ, was extracted from the working curve constructed by Nicholson using ΔEp values. The standard heterogeneous charge-transfer rate constant, k_0, for a given electron transfer process was determined using the following equation:

$$\psi = \frac{k_0}{(\frac{\pi n F D \nu}{RT})^{1/2}} \quad \text{Eq. 3}$$

where n is the number of electrons transferred, *F* is the Faraday constant, *D* is the diffusion coefficient, *v* is the scan rate, *R* is the ideal gas constant and *T* is the temperature.[5, 6]

Parameters for chronoamperometry/bulk electrolysis experiments. Bulk electrolysis experiments were performed in a H-cell with a glass frit separator (Porosity =10-16 µm, Pine Research, USA) using a Bio-Logic SP 150 potentiostat/galvanostat. An active species concentration of 5 mM was used. Working electrode compartment contained 15 mL of the active species with 100 mM $[NBu_4][PF_6]$ in CH_3CN and counter electrode compartment had 15 mL of 100 mM $[NBu_4][PF_6]$ in CH_3CN. A Pt mesh working electrode and a Pt wire counter electrode were used. Bulk electrolysis experiments were carried out using the chronoamperometry techniques available in EC lab software suite at constant potentials, selected from CV.

Parameters for charge discharge experiments. Charge-discharge testing was conducted in a nitrogen filled glove box using a glass H-cell (Adams and Chittenden, USA) and a Bio-Logic SP 150 potentiostat/galvanostat. The electrolyte solutions used in charge-discharge experiments were 5 mM active species in 0.1 M $[NBu_4][PF_6]$ in CH_3CN. Each compartment of the H-cell was filed with 5.0 mL of the electrolyte solution. The compartments of the H-cell were separated by an AMI-7001 anion exchange membrane (~0.05 cm^2, Membrane International Inc., USA). Two graphite felt electrodes (2 × 1 × 0.5 cm, Fuel Cell Store, USA) were placed in the posolyte and negolyte chambers. Electrodes attached to Pt wire current collectors submerged in the electrolyte solutions (~0.5 cm). Membranes and graphite felt electrodes were soaked in electrolyte solutions for 24 hours before each experiment. A galvanostatic charge-discharge method was adopted using a charging current of 0.15 mA and a discharging current of 0.015 mA for each experiment. Charging voltage cutoffs were 2.7 V for **1-TiV$_5$**, and 1.9 V for **2-Ti$_2$V$_4$** The discharge cutoff potential was 0.1 V for both experiments. For the duration of the charge-discharge experiments, both half cells were stirring at approximately 1,000 rpm.

Method for measuring percent crossover. For each **1-TiV$_5$** and **2-Ti$_2$V$_4$**, an H-cell divided by an AMI-7001 anion exchange membrane was set up with one half containing 10 mL of 5 mM TiPOV-alkoxide in acetonitrile with 0.1 M $[NBu_4][PF_6]$ supporting electrolyte, while the other half was "blank", containing only the supporting electrolyte solution. Both halves of the H-cell were stirred at approximately 1,000 rpm for the duration of the experiments. Daily, 3 mL aliquots were removed and analysed with UV-vis to determine concentration. Aliquots were replaced following analysis. Three trials were conducted for each cluster, and the average percent crossover reported.

Figure S1. Bulk oxidation and reduction curves of **1-TiV$_5$**

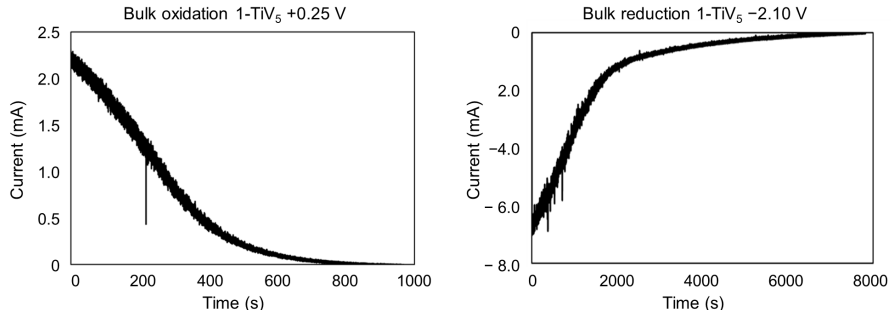

Figure S2. Color changes during bulk oxidation and reduction of **1-TiV$_5$**

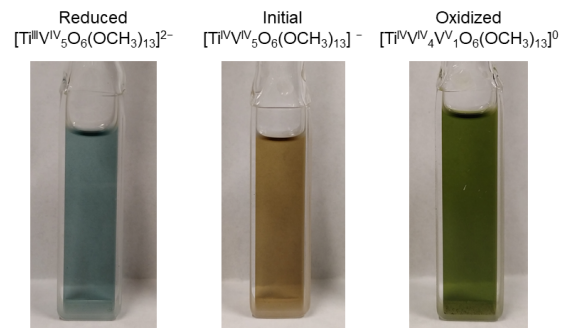

Figure S3. CV, UV-vis, monitoring of bulk oxidized and reduced solutions of **1-TiV$_5$**

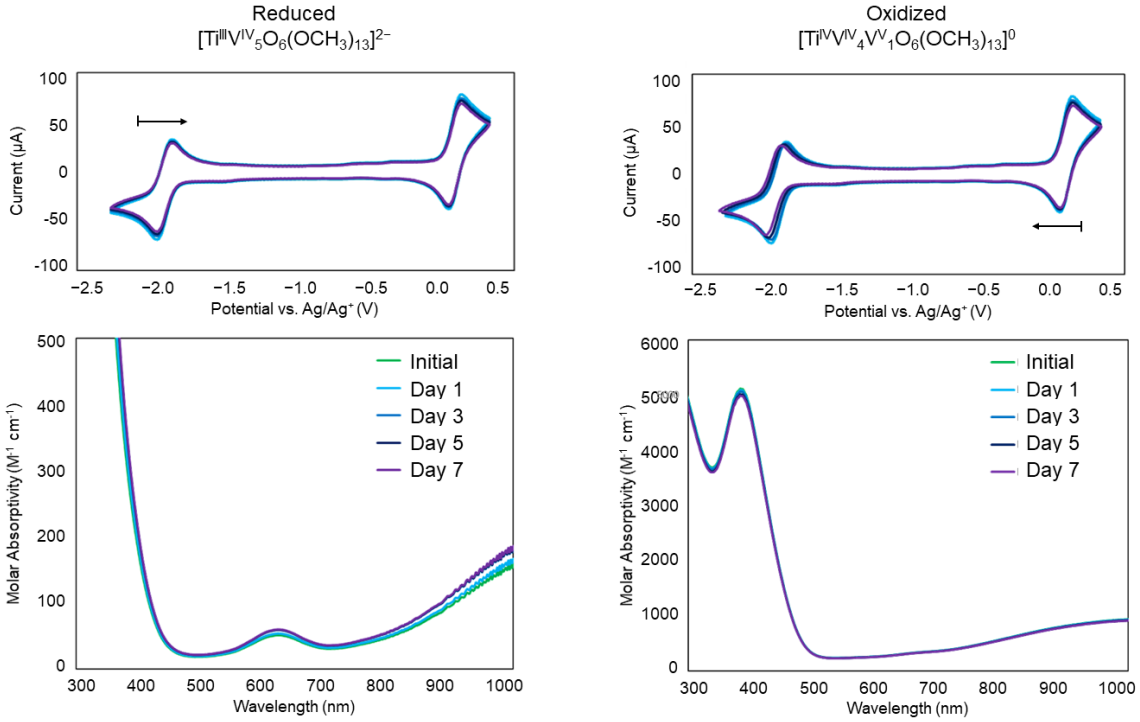

Figure S4. Bulk oxidation and reduction curves of **2-Ti$_2$V$_4$**

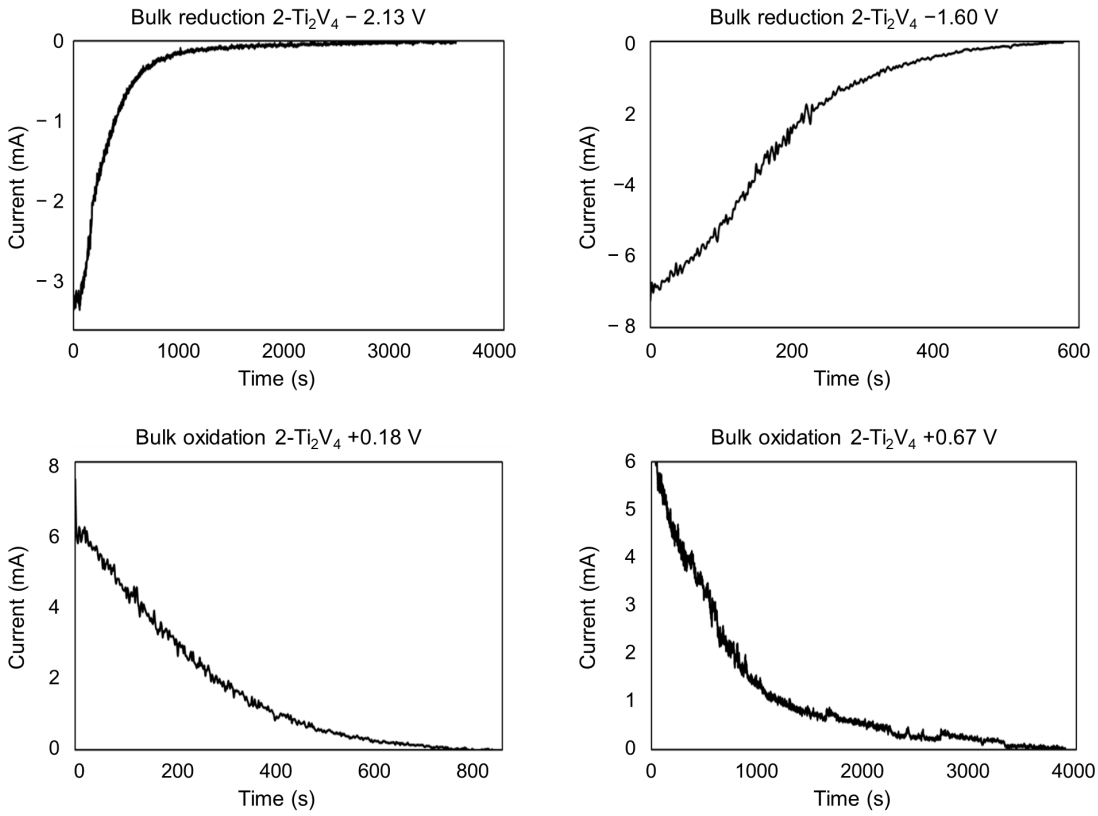

Figure S5. CV of **2-Ti_2V_4** following bulk oxidation (+0.67 V)

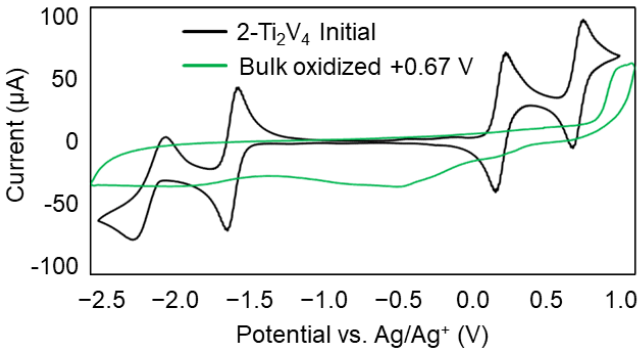

Figure S6. CV of **2-Ti_2V_4** following bulk reduction (−1.60 V)

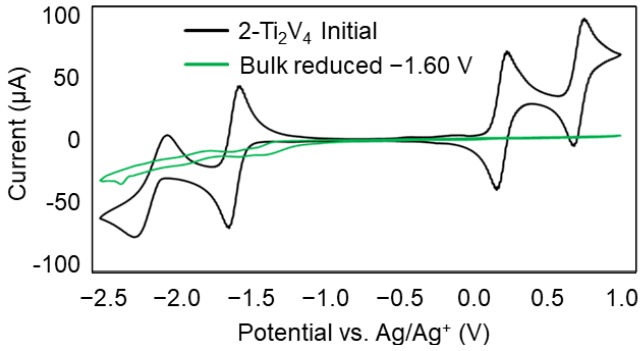

Figure S7. CV and UV-vis monitoring of bulk oxidized and reduced solutions of **2-Ti_2V_4**

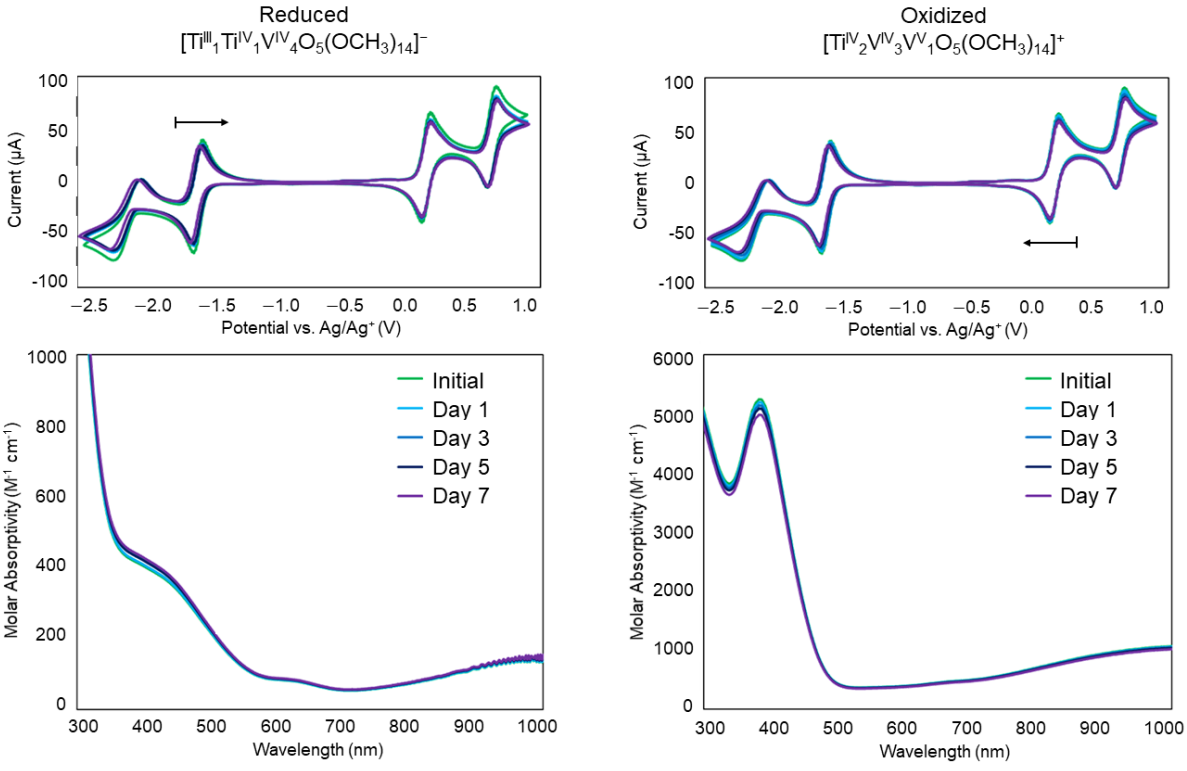

Figure S8. Plots of ΔE_p vs. scan rate for all redox events in **1-TiV$_5$** and **2-Ti$_2$V$_4$**. The increase in ΔE_p at higher scan rates for the titanium-based reduction events of both **1-TiV$_5$** and **2-Ti$_2$V$_4$** indicates quasi-reversible kinetics for each of these reduction processes (Figure 3a) In contrast, the ΔE_p is constant at all scan rates for the vanadium-based oxidation events, indicative of kinetically reversible electron transfer processes.

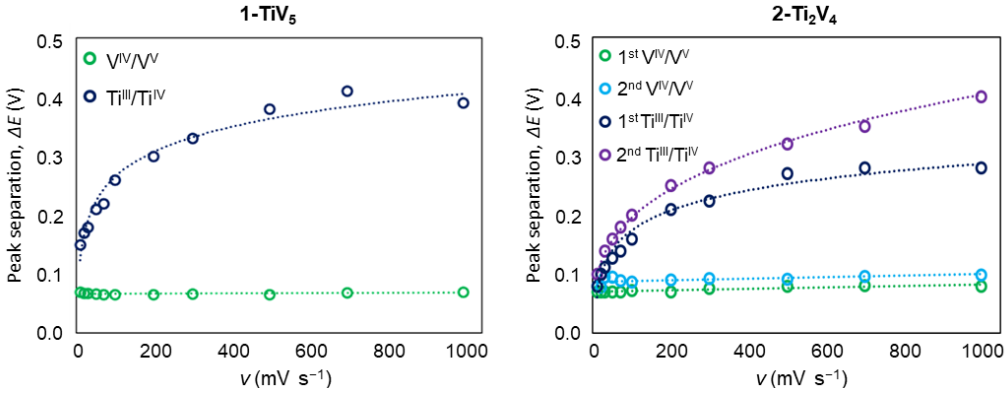

Figure S9. Solubility measurement of **1-TiV$_5$** in acetonitrile.

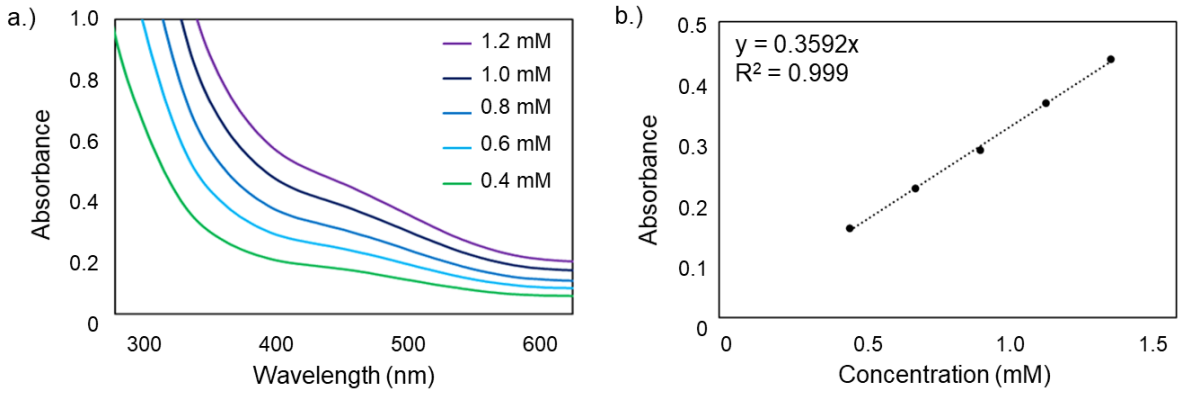

A 50 mM solution of **1-TiV$_5$** was diluted to concentrations between 0.4 mM and 1.2 mM, and absorption spectra obtained for each solution. Peak absorbance values at 452 nm were used to generate a calibration curve, with molar absorptivity, ε = 359.2 M^{-1} cm^{-1}. Three saturated solutions of **1-TiV$_5$** were allowed to stir overnight, and then 25 µL aliquots were removed and diluted to 10 mL. Concentrations of each saturated solution were calculated, and their average value determined to be 0.513 ± 0.005 M.

Trial	Absorbance at 452 nm	Diluted Concentration (mM)	Saturated Concentration (M)
1	0.4582	1.278	0.5103
2	0.4657	1.297	0.5186
3	0.4572	1.273	0.5091

Figure S10. Solubility measurement of **2-Ti_2V_4** in acetonitrile.

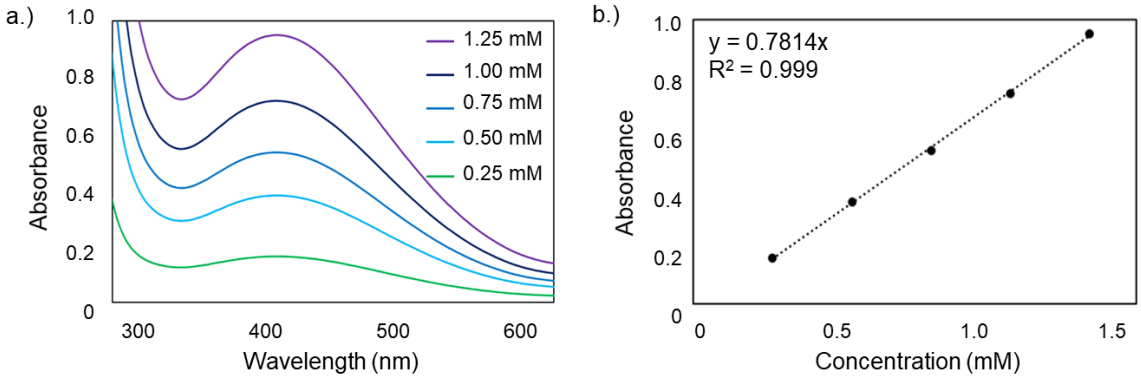

A 50 mM solution of 2-Ti_2V_4 was diluted to concentrations between 0.25 mM and 1.25 mM, and absorption spectra obtained for each solution. Peak absorbance values at 414 nm were used to generate a calibration curve, with molar absorptivity, ε = 781.4 M^{-1} cm^{-1}. Three saturated solutions of 2-Ti_2V_4 were allowed to stir overnight, and then 25 µL aliquots were removed and diluted to 10 mL. Concentrations of each saturated solution were calculated, and their average value determined to be 0.193 ± 0.009 M.

Trial	Absorbance at 414 nm	Diluted Concentration (mM)	Saturated Concentration (M)
1	0.3614	0.4625	0.1850
2	0.3706	0.4743	0.1897
3	0.3968	0.5078	0.2031

Figure S11. Absorption spectra for crossover experiments with (a) **1-TiV_5** and (b) **2-Ti_2V_4.**

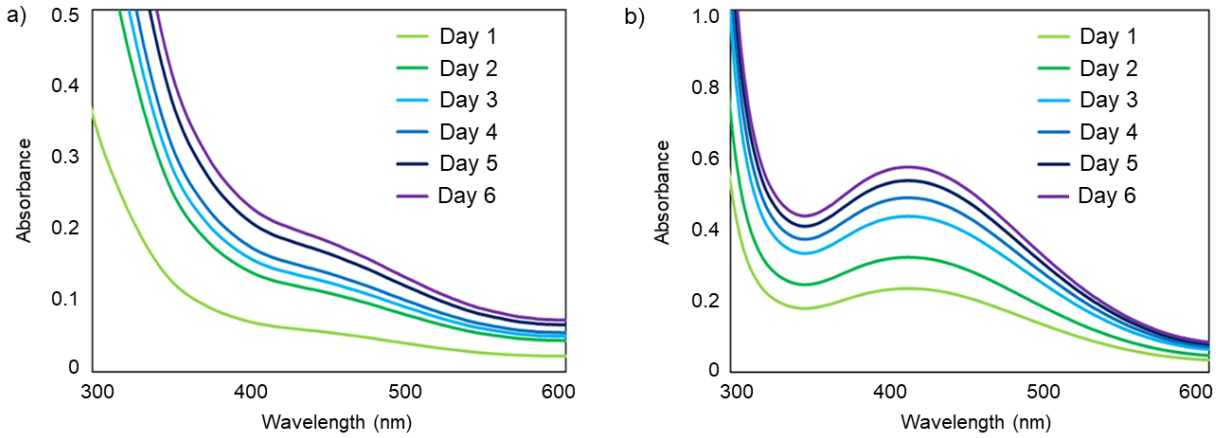

Figure S12. Full voltage trace of 2.7 V charge-discharge with **1-TiV$_5$**.

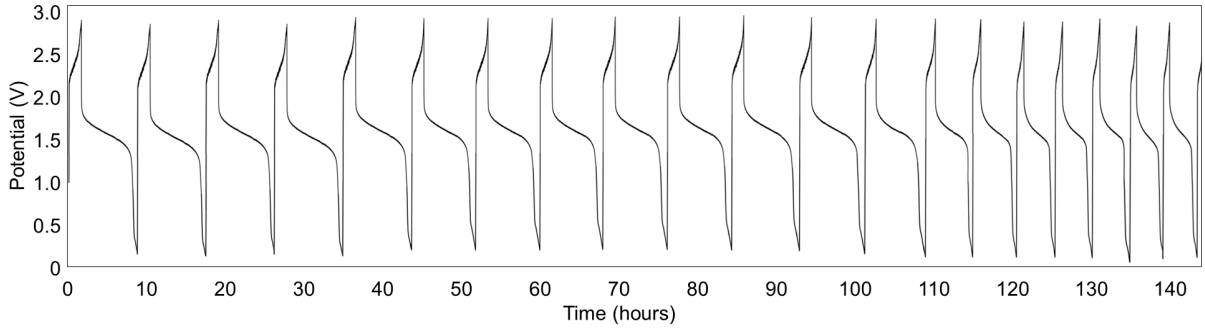

Figure S13. Charge capacity of **1-TiV$_5$** over the course of 20 cycles at 2.7 V.

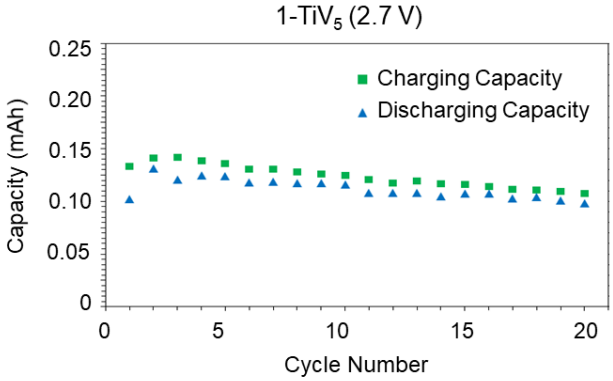

Figure S14. Full voltage trace of 1.9 V charge-discharge with **2-Ti$_2$V$_4$**.

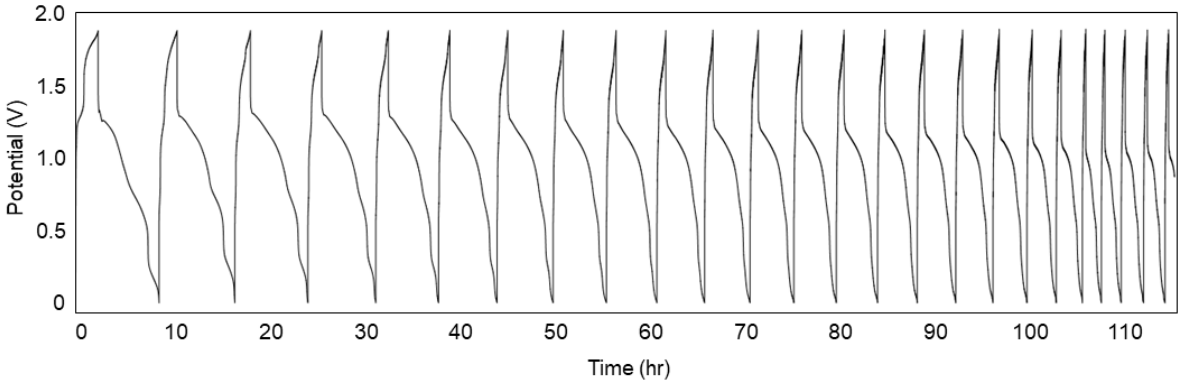

Figure S15. Charge capacity of **2-Ti_2V_4** over the course of 20 cycles at 1.9 V.

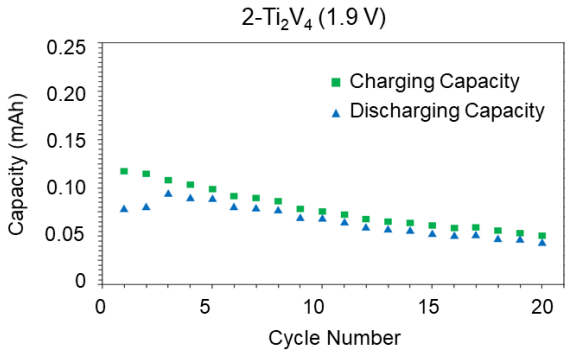

References

1. L. E. F. VanGelder, P. L.; Brenessel, W. W.; Matson, E. M., *Chemical Communications. Accepted*.
2. Q. Liu, A. E. S. Sleightholme, A. A. Shinkle, Y. Li and L. T. Thompson, *Electrochemistry Communications*, 2009, **11**, 2312-2315.
3. A. E. S. Sleightholme, A. A. Shinkle, Q. Liu, Y. Li, C. W. Monroe and L. T. Thompson, *Journal of Power Sources*, 2011, **196**, 5742-5745.
4. A. M. Kosswattaarachchi, A. E. Friedman and T. R. Cook, *ChemSusChem*, 2016, **9**, 3317-3323.
5. R. S. Nicholson and I. Shain, *Analytical Chemistry*, 1964, **36**, 706-723.
6. H. Muhammad, I. A. Tahiri, M. Muhammad, Z. Masood, M. A. Versiani, O. Khaliq, M. Latif and M. Hanif, *Journal of Electroanalytical Chemistry*, 2016, **775**, 157-162.